LESSONS LEARNED from the FUKUSHIMA ANALYSIS: THE MODELING OF SEVERE ACCIDENTS IN NUCLEAR POWER PLANTS

Luis E. Herranz, C. López, J. Fontanet, E. Fernández
Unit of Nuclear Safety Research, CIEMAT
Avda. Complutense 40, 28040 Madrid (Spain)
luisen.herranz@ciemat.es

ABSTRACT

The Fukushima accident is being both a unique opportunity and a huge challenge for severe accident analysis. Through the simulation of the accidents in Units 1 through 3 with MELCOR 2.1 scenarios have been postulated which outcomes look consistent with data. These analyses indicate that a massive core damage should have happened in Unit 1, with most core molten and located in the containment, whereas Units 2 and 3 core damage is anticipated to be much less. However, there might be differences among these "twin" units, since reactor vessel seems likely to have kept integrity in Unit 2, but it is not that likely in Unit 3. Anyway, in all the units the amount of H_2 produced is over 500 kg. Beyond specific results, sensitivity analyses on safety systems performance and prevailing boundary conditions have highlighted the need of conducting uncertainty analysis when modeling NPPs severe accident scenarios.

KEYWORDS
Fukushima; MELCOR code; uncertainties

1. INTRODUCTION

Severe accident analysis has undergone a deep and extraordinary evolution in the last 20 years. NUREG-1150 [1] was a milestone in Nuclear Power Plants (NPP) risk assessment. Five US NPPs were extensively analyzed with the Source Term Code Package (STCP), a suite of stand-alone codes which coupling allowed entire sequence simulation, from core degradation to source term to environment. About 20 years later, The State Of the Art Reactor Consequence Analysis (SOARCA) study reported what was considered "realistic outcomes of selected severe nuclear reactor accidents" in an attempt to address conservative aspects of previous reactor accident analyses [2]. To do so modern analysis tools were used. In addition to more extensive and better modeling of phenomena, the main change of these tools with respect to STCP was the move from code coupling to phenomena integration in a single computer code: MELCOR.

In spite of the outstanding progress, the SOARCA study acknowledged the need of conducting a comprehensive and integrated evaluation of modeling uncertainties, so that the report conclusions could be soundly supported. Such need has been even more highlighted in the light of Fukushima accident [3,4]. The progression of accident scenarios in Units 1 through 3 were drastically different, despite reactor similarity, and were highly dependent on two major uncertain aspects: safety system performance and actual boundary conditions at each unit.

This paper intends to highlight the two aspects introduced above: the current predictive capability of severe accident development and the sensitivity of the outcomes to key modeling factors. The Fukushima accidents in Units 1 through 3 have been simulated with the MELCOR 2.1 [5]. A summary of closer-to-data estimates achieved at the time are given with the focus on fuel degradation and thermal-hydraulics of Reactor Pressure Vessel (RPV) and Primary Containment Vessel (PCV). In addition, sensitivity studies to

major unknown aspects affecting accident unfolding have been shown. In the end all the results presented in the paper are discussed within the broad scope of the current predictability of severe accidents.

This work has been carried out in the frame of OECD-BSAF [6] project and some of the insights here reported have benefited from the discussion held.

2. ANALYSIS OVERVIEW

This section gives a brief account of the closer-to-data predictions found so far in the analyses of the Fukushima accidents in Units 1 through 3. The scope of the analyses has been limited to thermal-hydraulic aspects, and the target variables chosen have been pressure within both the RPV and the PCV. The time origin in the figures is the reactor scram when the units were hit by the quake. It should be underlined that these analyses have been called hereafter "Best Estimates" (BE), even though upcoming research coming up with new data concerning the units' state might result in refining the current models and, as a consequence, new scenarios could be postulated. In order to facilitate scenarios understanding, an overview of the main bases of the analyses are described next.

The analyses have been conducted with MELCOR 2.1 [5]. MELCOR is a fully integrated, engineering-level computer code that models severe accidents progression in light water reactors. It includes a broad spectrum of phenomena, from core degradation to source term to the environment. In most of models activated, default options have been taken, except for a number of cases that will be highlighted next.

2.1. Plant Nodalization

All of the Fukushima units have been meshed identically. A total of 65 compartments have been used to describe RPVs (38 volumes) and PCVs (27 volumes). Additionally, a few more cells have been added to consider the Reactor Building (RB).

The RPV has been split as shown in Fig. 1 (CVH nodalization): steam-dome, dryers, separators, shroud dome, annulus, lower plenum and 32 volumes for the core active region. In each radial node, the fuel channel inside the canister and the by-pass region (i.e., volume between adjacent canisters and water rods in fuel assemblies) are distinguished. The fuel channel has been axially split into 7 nodes to better capture axial thermal gradients, whereas just a single node has been used for the bypass. In addition to this thermal-hydraulic splitting, MELCOR requires a specific nodalization to track fuel degradation (COR nodalization). For this purpose, the core has been divided into 4 radial channels (a fifth one defined for the lower plenum zone under the downcomer). Axially the core has been meshed in 8 nodes, an additional one for the core plate and 3 more nodes describing the lower plenum of the RPV.

The PCV nodes have been distributed as follows (Fig. 2): 9 nodes for the Dry Well (DW), 8 circumferential nodes for the Wet Well (WW) and 8 more nodes for the vents in between DW and WW (i.e., the choice of 8 circumferential nodes is not arbitrary; it corresponds to the number of vents connecting DW and WW). In the DW, 3 regions have been considered in the axial direction and 2 in the circumferential one; only the central cylindrical region has considered two radial regions. One more volume has been kept for the cavity under the RPV. Each WW circumferential compartment has been connected to DW through a vent and a vacuum breaker (modeled as a valve-controlled flow path).

WW nodalization and flow path definition in between WW nodes are particularly relevant in this study. MELCOR assumes mass and energy discharged in the Suppression Pool (SP) immediately and uniformly distributed in the receiving control volume, which is quite an assumption for a body of water as large as the one in the SP when there is a single Safety Relief Valve (SRV) delivering steam (H_2O_v) and hydrogen

(H_2) from the vessel. This is even more significant in sequences with no power (i.e., SBO), as the Residual Heat Removal (RHR) system is not available and the induced water motion in SP is lost.

In case of RPV failure Molten Corium Concrete Interaction (MCCI) has been modeled as 3 interconnected cavities defined *ad-hoc*, one of which is the pedestal region and the other 2 correspond to the DW floor outside the pedestal.

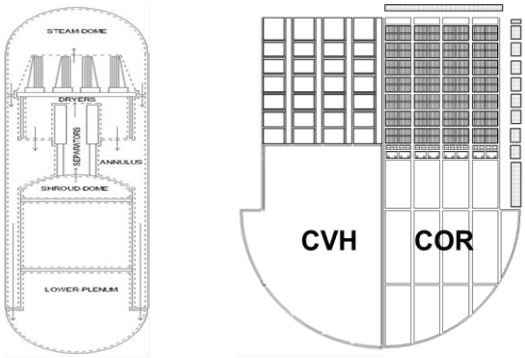

Figure 1. RPV nodalization.

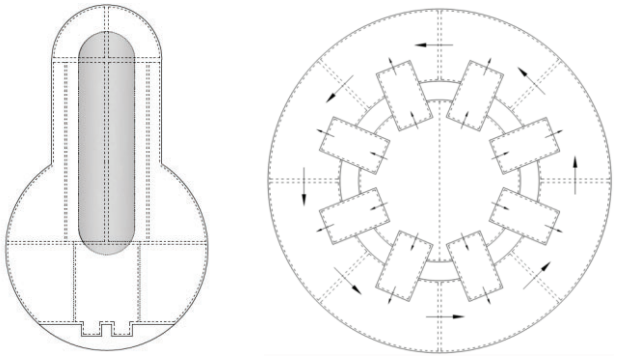

Figure 2. PCV nodalization.

2.2. Major Approximations

A key point in the modeling has been those approximations made concerning systems performance. Given the lack of accurate information, safety systems operation has been defined striving for the best fit possible to accident signatures, whenever the proposals made were physically defendable. Note that this extends also to vents, external water injections and leakages from RPV and PCV. Tables I-III synthesize the bases of the approximations made in each unit.

Table I. Unit 1 major approximations on systems performance

	System	**Approach**	**Practical application**
RPV	IC	Withdrawal of latent heat from dome	Fitted to capture P_{RPV}
	SRVs	Relief and safety modes	Setpoints of Unit 1
	External water injection	Source into the RPV downcomer	Fitted to capture P_{PCV}
	Leaks	SRV gasket failure into DW	$A=3.25\cdot10^{-3}$ m^2 (if T>723 K)
PCV	Vents	To environment	$A=1.6\cdot10^{-2}\cdot A_{vent}$ (if 23.2 h≤t≤24.2 h) $A=a(t)\cdot A_{vent}$ (if t>24.2 h)
	DW leaks	To RB	$A=f(P_{PCV})$ (if P>0.75 MPa)

A, cross section

Table II. Unit 2 major approximations on systems performance

	System	**Approach**	**Practical application**
RPV	RCIC	Water source in downcomer Steam and water sink in dome	Fitted to capture P_{RPV}
	SRVs	Relief and safety modes Manual actuation	Setpoints of Unit 2 Known operator action
	External water	Source into the	Fitted to capture P_{PCV}

	injection	RPV downcomer	
	Leaks	SRV gasket failure into DW	$A=5.0\cdot10^{-4}$ m^2 (if T>723 K)
PCV	DW leaks	To RB	$A=f(P_{PCV})$ (if P>0.75 MPa) $A=2.7\cdot10^{-3}$ m^2 (if t>88.5 h)
	Sprays	In WW	Known mass flow rate
	Torus room	Flooding after tsunami	Flooding rate to fit P_{RPV}
	RCIC exhaust	Source into WW	2-phase mixture ($0\leq x\leq 0.5$)

x, steam quality

Table III. Unit 3 major approximations on systems performance

	System	**Approach**	**Practical application**
RPV	RCIC	Water source in downcomer Steam sink in dome	Fitted to capture P_{RPV}
	HPCI		
	SRVs	Relief and safety modes ADS actuation	Setpoints of Unit 3 Known operator action
	External water injection	Source into the RPV downcomer	Fitted to capture P_{PCV}
	Leaks	SRV gasket failure into DW SRV leak into DW TIP failure	$A=1.5\cdot10^{-4}$ m^2 (if T>723 K t>41.7 h) $A=2.3\cdot10^{-4}$ – $1.4\cdot10^{-3}$ m^2 (if t<30 h) $A=4.2\cdot10^{-5}$ m^2 (if t>44.6 h T>1300 K)
PCV	DW leaks	To RB	Modeled but not activated
	Sprays	In DW and WW	Known mass flow rate
	WW vent	To environment	$A=4.0\cdot10^{-3}$ – $7.9\cdot10^{-3}$ m^2
	RCIC/HPCI exhaust	Source into WW	Saturated water (vapor assumed to reach the WW already condensed)

2.3. Major Results

In this sub-section the best fits to data for the time being (BE) have been presented and discussed.

2.3.1. Unit 1

Scarcity of data during the first 12 h is the main accident signature of Unit 1. As a consequence, there are a number of scenarios that might match the very few P_{RPV} and P_{PCV} data points existing until 12 h. Some of them have been screening out based on the cross-correlation of both variables, so that in essence the main hypotheses taken in the case results presented below are: SRV gasket failed at T>723 K is the only steam pathway (other than SRV discharge into the SP) to PCV; and an axial stratification in SP water might have happened, so that water layer below the SRV injection spot is not accounted for in the analysis. According to the modeling, just one SRV worked and it did on the relief mode until the tsunami made all power sources unavailable; from then on, it switched to the safety mode.

Fig. 3 shows in-RPV pressure along time with major events highlighted (external water injection has been noted by shadowing the corresponding time interval). According to the analysis, RPV would have maintained integrity till around 12 h, at which high temperatures caused penetration tubes failure. Core uncovery started at 2.8 h and temperatures kept on the rise at ~0.3 K/s until about 4 h; then, upon touching the 1500 K threshold, Zry oxidation speeded up (oxidation runaway) and temperature increase rate got to near 0.8 K/s; molten material relocation started and at RPV failure most of core materials had slumped into the Lower Plenum (LP) and were eventually ejected into the cavity more than 3 h later.

Fig. 4 displays PCV pressure evolution along the whole the time domain analyzed. As shown, during the first 4 hours P_{PCV} grows progressively as a consequence of PCV heat-up; at about 4.5 h, the H_2 generated by the cladding oxidation governs a fast increase of P_{PCV} that ends up at about 6 h. From this time on, steam and H_2 leaked through the SRV gasket become the main contributors to pressure rise until 12 h. At that moment, RPV rupture causes the peak observed at 12 h, at which P_{PCV} exceeded PCV upper head bolts pressure (0.75 MPa [7]) reaching practically 0.9 MPa. Corium gets to the cavity at about 15.3 h and the pressurization caused by the MCCI and the leaking from the PCV upper head seal drew a pseudo steady state; this was held until about 23.2 h, when WW venting became operational. It is worth mentioning that WW venting was intended to be closed later but it is assumed that it remained open with a variable cross section increasing from 9% of the vent piping to 13% (at t>50 h).

During the in-vessel phase of the accident, 750 kg of H_2 were produced (more than 80% from Zry oxidation). The total amount of combustible gases produced during the entire sequence is around 7000 kg. However, this number is uncertain and some additional studies are being conducted; thus no credit is given to it yet. As for degraded mass distribution, Table IV summarizes amounts and location of fuel and major structural and control rod materials in the Unit.

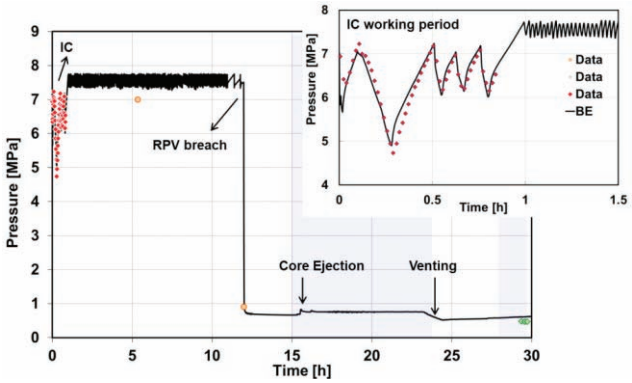

Figure 3. Unit 1 RPV pressure.

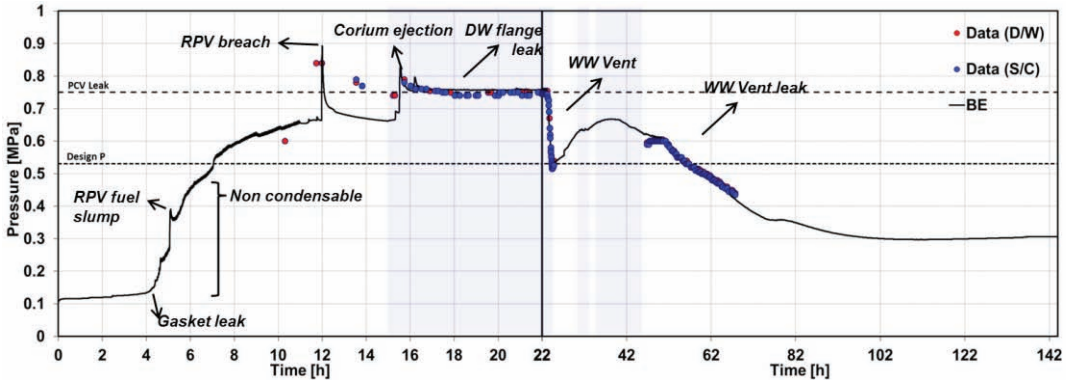

Figure 4. Unit 1 PCV pressure.

Table IV. Degraded mass (kg) distribution in Unit 1

	Initial mass (t=0 h)	Intact Mass (t=144 h)	Degraded Mass (t=144 h)		
			Mass in core	Mass in LP	% ejected
UO_2	76738	0	0	1	99.99%
Zr	31623	0	21	66	56%

		185 (as ZrO_2)	0 (as ZrO_2)	0 (as ZrO_2)	43% (as ZrO_2)
SS	38675	11400 1148 (as SS_{ox})	838 166 (as SS_{ox})	2059 367 (as SS_{ox})	56% 2% (as SS_{ox})
B_4C	700	58	0	0	92%
Total	147736	12791	1025	2493	89%

2.3.2. Unit 2

Contrary to the previous one, Unit 2 pressure recording was rather comprehensive of RPV and PCV evolution. One of the most outstanding features of Unit 2 is the Reactor Core Isolation Cooling (RCIC) performance under off-nominal conditions for nearly 70 h. This required assumptions concerning withdrawals from RPV dome and, no less important, the water state when entering the SP (not necessarily saturated water but a 2-phase fluid of variable composition). The RPV failure assumed is similar to Unit 1's (i.e., SRV gasket). The other highly uncertain boundary condition concerned the torus room flooding, which rate was fitted to follow PCV pressure for the first 70 h. As in Unit 1, just one SRV worked on the safety mode once RCIC failed.

Fig. 5 shows in-RPV pressure along time with major events highlighted (external water injection shadowed the corresponding time interval). Three major drivers govern P_{RPV}: decay heat, SRVs actuation and RCIC performance. For the first 65 h RCIC performance dominated RPV status (except for the first 5 h in which the SRV valve controlled RPV pressure). Pressure decreased with a noticeable slope from 5 to 15 h and then, once RCIC started sucking from WW water, pressure got back to levels around 6 MPa and decayed slowly according to the residual decay. RCIC unavailability made P_{RPV} increase sharply from around 68 h up to reaching the safety setpoint of the SRV. At around 75 h the SRV was manually opened and P_{RPV} dropped fast to 0.5 MPa; from that time until about 83 h, SRV opening/closing determined the observed pressure spikes. The reason behind a so good match of pressure after SRV manual actuation is closely related to the gasket failure assumed.

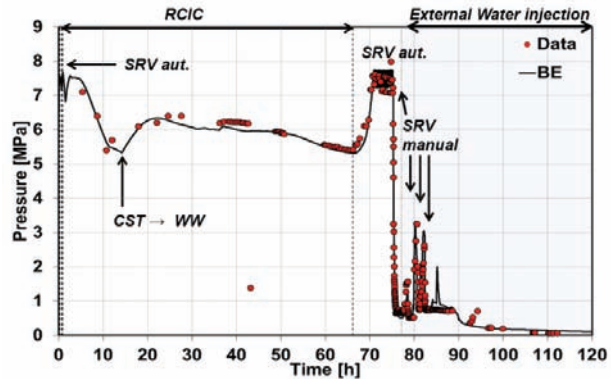

Figure 5. Unit 2 RPV pressure.

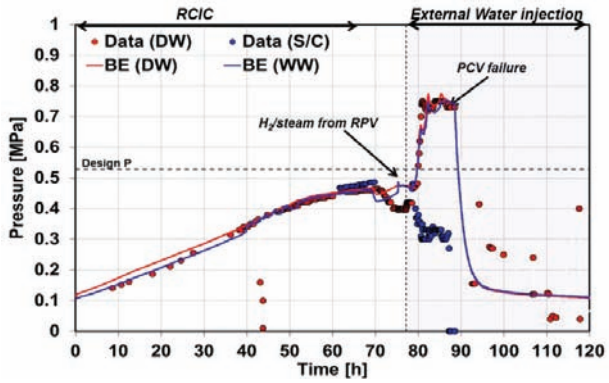

Figure 6. Unit 2 PCV pressure.

One noticeable difference with respect to the accident in Unit 1 is that according to the analysis, fuel deterioration was substantially less. Fuel has been predicted to start degrading at around 77 h and, as residual power after about 3 days was notably less, it proceeded at a much slower rate (temperature increases rates were around 0.2 K/s, 4 times less than in Unit 1). This fact together with the effective external water injection at about 81 h, made core damage be much less extensive and practically restricted to the central region of the core (rings 1 and 2 in the modeling). As a consequence, RPV did not fail.

Fig. 6 displays PCV pressure evolution. During nearly 70 h a quasi linear pressure increase was measured and predicted; this progressive pressurization seemed to be related to the continuous heat up due to natural convection from RPV surfaces and SP water warm up due to RCIC exhaust. At around 40 h a slight change in WW pressure that drives it to the DW one is noted; the reason behind is the SP water saturation that makes steam reach WW atmosphere and open the vacuum breakers to move up to the DW. From 70 h on, WW data are not reliable and PCV pressure signature is just given by the DW one. As observed, the fast pressure rise to near 0.75 MPa, responds to steam and H_2 injection coming directly from SRV gasket. The next steady state at that pressure resulted from the PCV head flange failure at 0.75 MPa. The final P_{PCV} pressure drop was postulated as a loss of integrity of PCV at 88.5 h.

During the accident 600 kg of H_2 were produced (more than 93% from Zry oxidation). As for degraded mass distribution, Table V summarizes how fuel and other materials distribute in the Unit; as said above, RPV kept integrity so that no corium was ejected in the pedestal.

Table V. Degraded mass (kg) distribution in Unit 2

	Initial mass (t=0 h)	Intact Mass (t=144 h)	Degraded Mass (t=144 h)		
			Mass in core	Mass in LP	% ejected
UO_2	106800	54800	2500	49500	-
Zr	43800	2900 4700 (as ZrO_2)	1500 800 (as ZrO_2)	27000 6900 (as ZrO_2)	-
SS	49900	47190 250 (as ZrO_2)	540 45 (as SS_{ox})	1520 360 (as SS_{ox})	-
Total	200500	109835	5385	85280	-

2.3.3. Unit 3

As in Unit 2, RPV and PCV pressure measurements in Unit 3 were frequent enough as to provide a full description of accident evolution. Actuation of the High Pressure Coolant Injection (HPCI) and Automatic Depressurization System (ADS) resulted in broad oscillations of RPV pressure, so that the entire accident may be described in pressure periods. As for containment, multiple venting heavily conditioned the long run (after around 40 h) evolution of pressure.

Fig. 7 shows that during around 20 h, SRV and RCIC actuation kept RPV pressure at the upper level of the safety function of SRVs (roughly, 7.8 MPa). At 21 h the transition to HPCI (with a nominal flow rate about 10 times RCIC's one), led to an effective depressurization of the system down to around 1.0 MPa, pressure below the optimum working range of the HPCI turbine-driven pump. It is assumed to cause the interruption of water supply to RPV (31 h), which resulted in RPV water level decrease. At around 36 h HPCI was manually stopped and core uncovery started and rapidly got back to high pressure levels (over 70 bar) due to steaming and hydrogen generated mostly from Zry oxidation. SRVs came into operation again until at around 42 h the ADS was activated, so that RPV pressure plunged and made it feasible external water injection; from that time on RPV and PCV pressures evolved similarly. Fuel degraded at a gentle rate (0.1 K/s) until about 40 h at which the chemical enthalpy from the oxidation reactions speed up the core-heat-up. Even though fuel damage was estimated to be extensive (nearly 50%), no RPV failure was predicted.

Several phenomena contributed to the PCV pressure (Fig. 8) during the first 20 h. DW atmosphere heated-up by natural convection from RPV walls. Steam injection in the SP through SRVs and through

RCIC turbine resulted in temperatures at or near saturation for quite some time during this first 20 h in the receiving pool node; this meant that a fraction of all the steam entering the pool in the 20 h time span did not condense in the SP and got eventually in the PCV atmosphere. The third non-negligible contribution was a direct ingress of steam in the DW (associated to SRV piping). Then, pressure water spraying in DW and WW and loss of steam sources in PCV (SRVs at about 21 h; HPCI at around 30 h) relieved PCV pressure until little earlier than 40 h, time at which P_{PCV} reacts again to RPV pressurization through SRVs operation and the associated leaking to the DW. From 42.5 h on, P_{PCV} is determined by vents and the external water injection. Metal oxidation (mainly Zr, 90%) produced more than 1000 kg of H_2. As for degraded mass distribution, Table VI summarizes amounts and locations of major in-core materials.

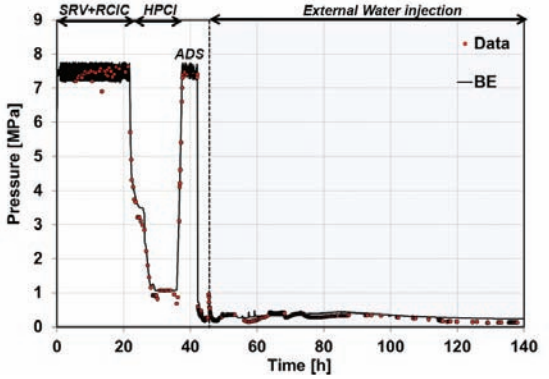

Figure 7. Unit 3 RPV pressure.

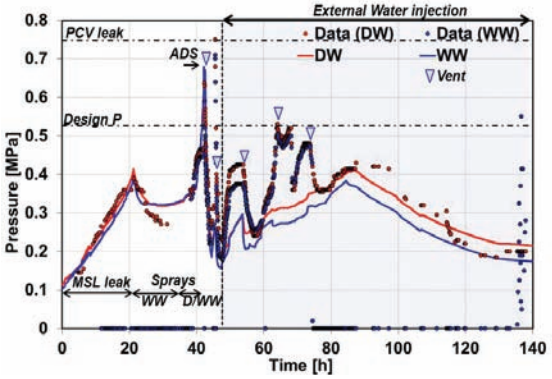

Figure 8. Unit 3 PCV pressure.

Table VI. Degraded mass (kg) distribution in Unit 3

	Initial mass (t=0 h)	Intact Mass (t=144 h)	Degraded Mass (t=144 h)		
			Mass in core	Mass in LP	% ejected
UO_2	106800	55630	870	50300	-
Zr	43800	3529 7961 (as ZrO_2)	4740 2920 (as ZrO_2)	13900 10750 (as ZrO_2)	-
SS	49900	34168 32 (as SSox)	3280 1480 (as SS_{ox})	10050 890 (as SS_{ox})	-
Total	200500	101320	13290	85890	-

3. SENSITIVITY ANALYSIS

The previous section has summarized the major insights gained into the accident evolution of Units 1 through 3 of Fukushima Daiichi. Nevertheless, the results obtained are tightly subject to a number of hypotheses, approximations and assumptions made in the modeling. In order to assess how sensitive the MELCOR outputs are to specific features of the model in which the user can make a noticeable difference, some sensitivity calculations have been done and classified next in: systems modeling and boundary conditions.

3.1. Systems Modeling

This section explores the effect of the approach adopted in modeling two key features of Mark I containment: WW and reactor cavity. Both of them require modelers to make a good number of assumptions, often concerning uncertain parameters of major influence.

3.1.1. WW nodalization

Nuclear reactors nodalization has been demonstrated to largely affect modeling of a number of phenomena, like in-containment hydrogen distribution [8], gaseous iodine-steel interactions [9] or WW pool stratification [10] among many others. The latter might be of particular significance in Boiling Water Reactor (BWR) accident scenarios since the thermal state of SP affects the peak containment pressure and, if existing (depending on BWR designs) and available, the performance of safety systems, like the RCIC and HPCI. A number of previous analyses assumed a simple containment nodalization when analyzing accidents in BWR Mark I NPPs [11, 12] and even some recent works [13] seem to follow that path. However, this is a strong hypothesis which impact is worth to be further investigated.

The study has been focused on Unit 1 and it consisted of 3 cases:

- A single-cell nodalization (WW 1 node); this approach involves an instantaneous thermal homogenization of SP water or, in other words, the maximum heat capacity that SP water can have (i.e., $m_{pool} \cdot c_p$) and, as a consequence, the minimum chance for water to reach saturation.
- A WW splitting into 8 circumferential nodes (WW 8 nodes); this arrangement makes water in the SRV discharging node more prone to saturation, as water heat capacity is reduced in a factor proportional to the number of meshes done.
- An 8 compartments discretization of WW neglecting water below injection (BE); this means that water below the SRV injection spot does not play any role in the scenario (i.e., "perfect axial stratification"). This would be the case with less thermal inertia of the pool at the injection node.

As observed in Fig. 9-10, within the proposed scenario, any nodalization scheme explored out of the one considered in the BE worsens data-predictions consistency, postponing RPV failure for nearly 2 h and showing noticeable differences with PCV measurements from 10 to 20 h. It should be highlighted that the alternative nodalizations proposed do not exceed PCV failure pressure until about 20 h, whereas data over 0.75 MPa were recorded near 12 h. Anyway, the MELCOR responses to the new nodalizations seem to be coherent with the larger thermal inertia of both cases compared to the one of the best fit. In fact, the source of the differences observed is directly related to the thermal state of SP, which is significantly closer to saturation in the closer-to-data case (BE) than in the other two calculations. It is noteworthy that such a different saturation state of water would also affect the scrubbing efficiency of SP when fission products and aerosols are considered, underlining differences of these three cases. Despite differences noted, when looking at total H_2 produced or degraded mass, no major discrepancies have been found. Finally, it is also worth mentioning that a better match to the measured pressure could have been obtained for each WW nodalization if changing the sequence. In such cases, the pool's thermal state should also be analyzed.

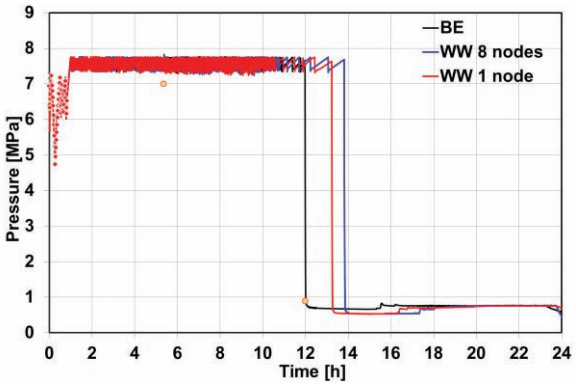

Figure 9. Unit 1 WW nodding (P_{RPV}).

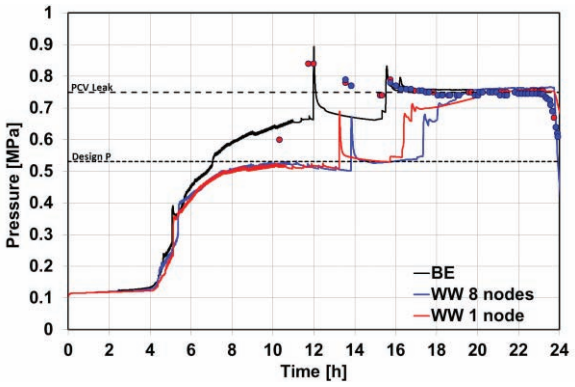

Figure 10. Unit 1 WW nodding (P_{PCV}).

3.1.2. Reactor cavity

In case of RPV failure molten materials fall in the reactor cavity at very high temperatures. The MCCI can result, directly or indirectly, in PCV failure by several mechanisms: over-pressurization, base mat penetration, generation of combustible gases increasing the chances for deflagration/detonation and, in the particular case of Mark I containments, liner melt-through [1]. Thermal concrete decomposition produce H_2O and CO_2 that bubble through the pool of molten materials; on their way to the surface they oxidize embedded metals and turn into H_2 and CO, both of which are combustible gases. The gas motion through corium results in fission product and aerosol transport to the molten pool surface, from which they can be transferred to the gas phase and, hence, increase the potential source to the environment. Beyond the suitable definition of initial conditions and proper physical modeling in codes, reactor cavity modeling (i.e., noding of DW bottom, material transfer between cavity rooms, corium spreading rate, etc.) is certainly crucial for accidents with ex-vessel phase (i.e., loss of RPVV integrity) and it is a huge challenge for the modeler due to the large effect of the variables that need to be defined

As in the previous section, the study has been focused on Unit 1 and it consisted of 3 cases (Fig. 11):

- A single cavity (1 CAV); molten materials fall and remain within the reactor pedestal boundaries until cavity failure (if it ever happens).
- Two cavities (2 CAV); molten materials fall in the reactor pit and, it can be partially transferred outside whenever they pile up more than 0.1 m over the upper level of materials in the receiving cavity; the mass fraction (x_m) transferred is thermally controlled: if $T < T_{solidus}$ (1350 K)$\rightarrow x_m = 0.0$; if $T_{solidus} \leq T \leq T_{liquidus}$ (1650 K)$\rightarrow x_m = \frac{T - T_{solidus}}{T_{liquidus} - T_{solidus}}$; if $T > T_{liquidus} \rightarrow x_m = 1.0$. The material spreading rate assumed has been $2.2 \cdot 10^{-3}$ m/s [7].
- Three cavities (3 CAV, BE); similar to the 2 CAV case, but the volume out of reactor cavity is split in 2 cells; the conditions for mass transfer between cavities are the same as in 2 CAV, but an instantaneous uniform spreading in the receiving cell is assumed (default MELCOR option).

Fig. 12 shows a substantial difference between the 1 CAV case and the other two. The reason behind is the code stops once pedestal is entirely ablated (at around 20 h). As said in section 2.3.1, estimates of gas production during the ex-vessel phase are not given any credit yet, as they might result from a numerical problem when solving implicitly some of the MELCOR equations [14]. Even so, the study is still useful to assess the sensitivity of results to cavity modeling: noticeable differences can show up in combustible gas production depending on the cavity model approach (Fig. 12). However, those discrepancies would not entail significant changes in the scenarios (Fig. 13): the amount of combustible gases produced is quite a lot anyway and, given that containment pressure after 20 h is heavily affected by PCV failure and venting, it can still be captured by imposing fitted boundary conditions once the molten materials fall into the cavity.

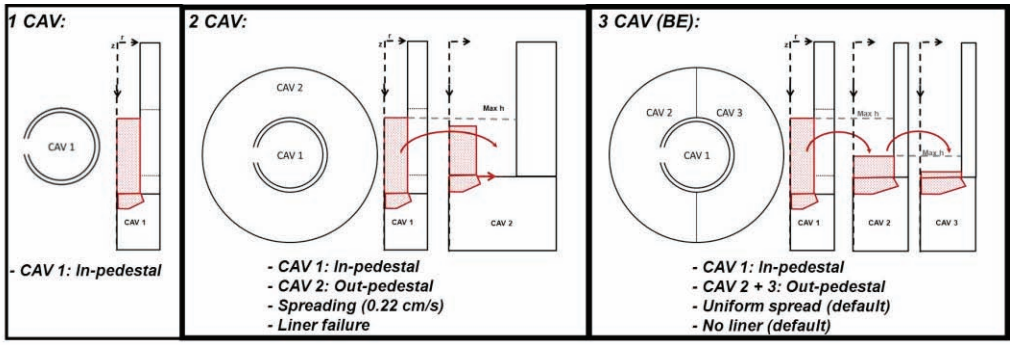

Figure 11. Unit 1 cavity models.

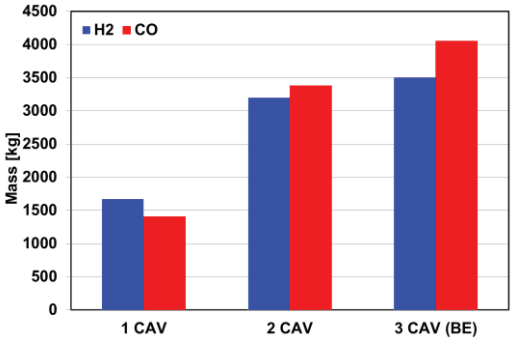

Figure 12. Unit 1 cavity model (gases).

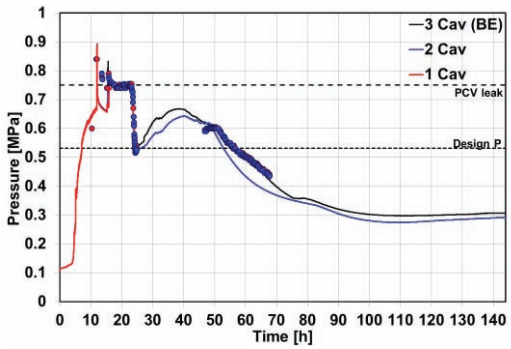

Figure 13. Unit 1 cavity model (P_{PCV}).

3.2. Boundary conditions

This section illustrates the impact of unknown key boundary conditions on code results. This is pretty much the situation of the forensic analysis of the Fukushima Daiichi accidents.

3.2.1. Safety systems performance

During the Fukushima accidents some cooling systems worked under off-nominal conditions. This was particularly the case of the RCIC and the HPCI systems in Units 2 and 3, respectively. Uncertainties in their operation range from mass flow rates of steam and water to their thermal state as individual fluids or as a 2-phase mixture reaching the SP. Sensitivity studies of RCIC and HPCI performances in Unit 2 and 3, respectively, have been conducted.

Fig. 14 shows the RPV pressure evolution in Unit 2 of three postulated performances of RCIC:

- Best Estimate (BE); this approach has been basically derived from an approximate solution of mass and energy equations. The resulting mass flow rates have been slightly corrected, though, to better capture P_{RPV} data recorded. The thermal states of water and steam have been assumed to be those at the dome for the suction point and saturated at turbine outlet conditions for the SP discharge (along the RCIC operation the fraction of water and steam delivered to the SP has been variable).
- Mass Flow Rates (MFR); this case adopts the same thermal state of water and steam and keeps mass flow rate as resulting from solving energy and mass conservation equations, without any correction.
- Thermal State (ThS); here the BE mass flow rates have been adopted, but water loss of enthalpy on the way from RPV to SP has been considered negligible, whereas steam gives off a fraction of enthalpy according to the nominal turbine efficiency.

It is worthy to note that in all the cases P_{PCV} estimates were consistent with measurements; this required imposing different flooding rates of the torus room.

As observed, slight changes in mass flow rates (BE vs. MFR) can result in losing the measured trends and in quantitative differences of more than 1.0 MPa at the end of the RCIC performance (~ 68 h). On the other side, when keeping the same mass flow rates and changing the fluids thermal state (BE vs. ThS), trends are maintained but deviations may be over 1.5 MPa in certain periods of time. These discrepancy bands can give an idea of uncertainties in case the modeler has no data available to streamline input deck assumptions. In terms of variables more directly linked to accident severity, like core degradation or H_2 produced, meaningless differences have been found, except for the MFR case, which produced about 150 kg of H_2 less than the BE (~450 kg).

Fig. 15 displays the RPV evolution in Unit 3 in the period of HPCI actuation. Two postulated performances of HPCI have been included with no other major changes that mass flow rates and deactivation of HPCI at 1 MPa in the BE. The basis to estimate mass flow rates has been in both cases resolution of energy and mass equations using the level measurements as a reference. However, the water injection used in the BE has been modified to better accommodate data trends, particularly at the start of HPCI working period (~22 h). The total mass of water injected has been kept roughly the same. Steam flow rates have been hardly changed. The change in P_{RPV} between 22 and 37 h is quite substantial. As a consequence of the different core cooling, hydrogen production grows around 20% (~1200 kg) and, more importantly, the total mass degraded exceeded 70% (nearly a factor 1.5 over BE).

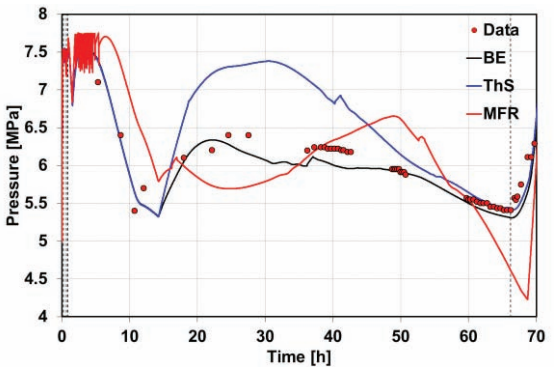

Figure 14. Unit 2 cooling systems (P_{RPV}).

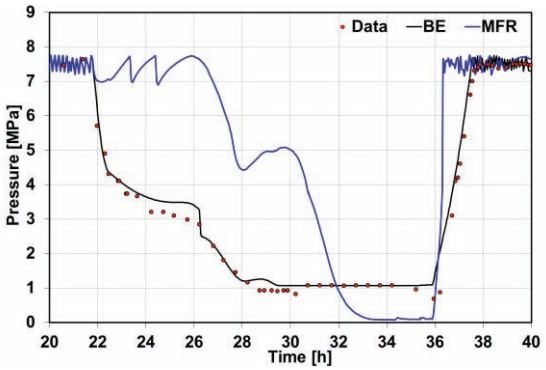

Figure 15. Unit 3 cooling systems (P_{RPV}).

3.2.2. Unexpected WW cooling

As a consequence of natural phenomena occurring at the site (i.e., quake and tsunami) the torus room of the units could have been flooded. Unfortunately, there is no information about it. Despite the absence of specific data, pressure rise in the Unit 2 PCV seemed too slow for storing all decay heat that was being transferred to SP through RCIC and SRV. Therefore, flooding of Unit 2 torus room seems to be an acceptable assumption [3]. In this case the modeler faces with a number of hypotheses to make, like the final water depth and the mass flow rate history; the latter might range from a fast flooding right after the tsunami arrival to a progressive flooding afterwards.

Fig. 16-17 show the RPV and PCV pressure evolutions in Unit 2 of three postulated scenarios for torus room flooding:

- No Flooding (NoFld); no water is assumed in the torus room so that SP is cooled by air natural convection.
- Fast Flooding (FFld); water is supposed to enter the torus room in 10 min after the tsunami arrival; namely, a more effective SP cooling is foreseen.
- Best Estimate (BE); torus room flooding starts about one day after the accident onset and progressively fills up to reaching the center of the WW.

As shown, RPV pressure undergoes substantial deviations after 15 h in the case fast flooding, as SP water temperature is colder than in the other two cases, whereas in the BE the progressive flooding results in an enhanced cooling only after water level at the torus reaches the bottom of the WW (~50 h). In short, outstanding discrepancies in RPV pressure of more than 2 MPa could result from different flooding rates. As for PCV pressure, it is after about 40-50 h when differences become significant and, as in RPV pressure, the case with no flooding cannot even follow the data trends.

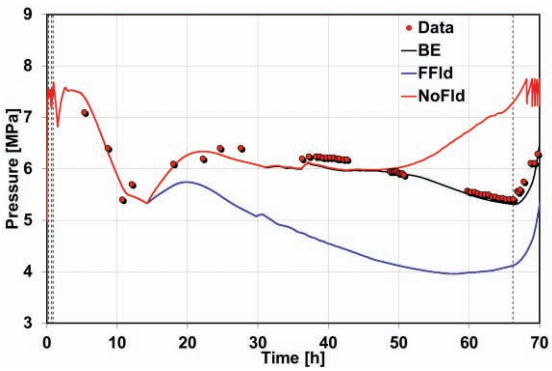

Figure 16. Unit 2 torus room flooding(P_{RPV}).

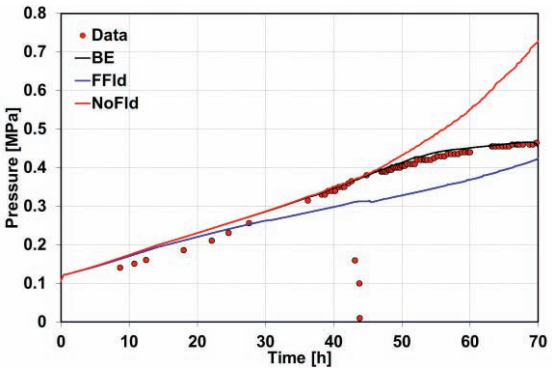

Figure 17. Unit 2 torus room flooding(P_{PCV}).

4. FINAL REMARKS

Severe accident simulation has undergone a huge progress in the last decades. However, the intrinsic nature of severe accidents (i.e., extreme conditions, tightly coupled phenomena, scaling, etc.), makes this research domain tough to be addressed even under international cooperation frameworks, like the OECD-BSAF project. Codes encapsulate knowledge in the form of models, many of which eventually rely on empirical factors, often based either on separate effect tests hard to be extrapolated to actual scale or derived from a "scaled" but scarce and incomplete data base. This turns codes application to NPPs into a far from straightforward task making severe accident modelers face with uncertainties in three major areas: plant description, phenomena modeling and boundary conditions specification. This idea was the main motivation for this article.

Scenarios of accidents in Units 1 through 3 of the Fuksuhima-Daiichi site have been postulated and the results obtained with MELCOR 2.1 have shown reasonable agreement with thermal-hydraulic data available. They allow setting two major conclusions:

- Substantial core damage seems to have happened in all the units, particularly in the Unit 1, where very likely RPV failed and molten materials found their way to PCV. Contrarily, the other 2 units might have kept RPV integrity. Nonetheless, whereas this is apparently a quite sound statement in Unit 2, it is not that heavily supported in the case of Unit 3, where long term pressure in PCV has not been captured as consistently as desired and slight changes of boundary conditions have proved to lead to RPV-failed scenarios.
- In all the units the production of H_2 was, at least, in the order of hundreds of kg. This means that in any of them, whether H_2 had found its way to the non-inerted RBs, it might have caused deflagrations and/or detonations, as it was the case in Units 1 and 3.

The current status of analyses, the associated uncertainties and the limited feasible comparisons to data, hinder any more detailed conclusions to be settled.

The scenarios proposed should be understood as plausible ones based on their consistency with data, but they should not be taken as the only existing possibilities to match the known footprints of the accidents. The sensitivity studies carried out addressed some uncertain features concerning systems performance and boundary conditions. Their results have provided a good illustration of how different MELCOR results could have been if other still reasonable assumptions in plant modeling had been done or if no data had existed to derive system performance specifications. No less important, some studies have shown that different modeling approaches could result in similar outputs by just modifying unknown boundary conditions. Access to more data might limit to some extent this "flexibility".
This study has led to some reflections concerning severe accident analysis, generally speaking:

- The importance of setting suitable goals for severe accident analyses of NPPs, striving for major footprints of scenarios instead of looking in detail at specific phenomena that are too sensitive to uncertain boundary conditions.
- The forcefully limited accuracy of results from NPP severe accident simulations given the necessary approximations made in plant description, phenomena modeling and postulated boundary conditions.
- The gain of robustness in major insights concerning accident progression and source term when a "full-scope" uncertainty analysis is conducted. If for any reason such analysis is not feasible, extensive sensitivity studies should be carried out.
- The absolute need for "well-focused" severe accident research that allows a global understanding of accident evolution by addressing, at the necessary level, essential phenomena for either progression and/or consequences of the accidents.

ACKNOWLEDGMENTS

The authors acknowledge all the partners of the OECD-BSAF Phase 1 project for the fruitful discussions and the Spanish Regulatory Body for their financial and technical support.

REFERENCES

1. US Nuclear Regulatory Commission, "Severe Accident Risks: an Assessment for Five US Nuclear Power Plants", NUREG-1150 (1990).
2. US NRC, "State-of-the-Art Reactor Consequence Analyses Report", NUREG-1935 (2012).
3. TEPCO, "Evaluation of the Situation of Cores and Containments Vessels of Fukushima Daiichi Nuclear Station Units 1-3 and Examination into Unsolved Issues in the Accidents. Report 2 (2014).
4. R. Gauntt, D. Kalinich, J. Cardoni, J. Phillips, A. Goldmann, S. Pickering, F. Matthew, K. Robb, L. Ott, D. Wang, C. Smith, S. St.Germain, D. Schwieder and C. Phelan, "Fukushima Daiichi Accident Study (Status as of April 2012)", Sandia Report SAND2012-6173 (2012).
5. SNL, "MELCOR Computer. Code Manual", NUREG/CR-6119, **Vol.1**, Rev 3179 (2011).
6. OECD/NEA, BSAF Project, https://www.oecd-nea.org/jointproj/bsaf.html
7. US Nuclear Regulatory Commission, "State-of-the-Art Reactor Consequence Analyses Project. Volume 1:Peach Bottom Integrated Analysis", NUREG/CR-7110, **Vol. 1** (2012)
8. S, Schwarz, K. Fischer, A. Bentaib, J. Burkhardt, J.J. Lee, J. Duspiva, D. Visser, J. Kyttälä, P. Royl, J. Kim, P. Kostka and R. Liang, "Benchmark on Hydrogen Distribution in a Containment Based on the OECD-NEA THAI HM-2 Experiment", *Nuclear Technology* **175**, pp. 594-603 (2011).
9. G. Weber, L.E. Herranz, M. Bendiab, J. Fontanet, F. Funke, B. Gonfiotti, I. Ivanov, S. Krajewski, A. Manfredini, S. Paci, M. Pelzer and T. Sevón, "Thermal-Hydraulic-Iodine Chemistry Coupling: Insights Gained from the SARNET Benchmark on the THAI Experiments IOD-11 and IOD-12", *Nuclear Engineering and Design* **265**, pp. 95-107 (2013).
10. L.E. Herranz, J. Fontanet, E. Fernández and C. López, "The Effect of Nodalization on the Wet Well's Performance during an SBO accident", *Proceedings of the 10th International Topical Meeting on Nuclear Thermal-Hydraulics, Operation and Safety (NUTHOS-10)*, Okinawa, Japan, Dec14-18 2014.
11. M. Lee and G.D. Lee, "Quantification of Severe Accident Source Terms of BWR4 Reactor With Mark I Containment Using STCP", *Nuclear Engineering and Design* **138**, pp. 313-337 (1992).
12. J.J. Carbajo, "MELCOR Sensitivity Studies for a Low-Pressure, Short Term Station Blackout at the Peach Bottom Plant", *Nuclear Engineering and design* **152**, pp. 287-317 (1994).
13. S-Y. Park and K-I. Ahn, "Comparative Analysis of Station Blackout Accident Progression in Typical PWR, BWR and PHWR", *Nuclear Engineering and Technology* **44(3)**, pp. 311-322 (2012).
14. C. López, J. Fontanet and E. Fernández, "Recent CIEMAT's Insights into MELCOR 2.1 Performance". *Proceedings of MCAP 2014,* Bethesda (Maryland, USA), September 18-19 (2014).